

## Supplementary Material

### **Phenanthroline-functionalized donor-acceptor covalent organic frameworks as photo-responsive nanozymes for visual colorimetric detection of isoniazid**

Guorong Li<sup>a,\*</sup>, Yixin Yang<sup>c</sup>, Wenjie Chen<sup>a</sup>, Zhiping Song<sup>d</sup>, Jiale Shi<sup>a</sup>, Bingqing Wang<sup>a</sup>,  
Xiaoyang Pan<sup>a,\*</sup>, Zian Lin<sup>b,\*</sup>

<sup>a</sup> College of Chemical Engineering and Materials Science, Quanzhou Normal University, Quanzhou, Fujian, 362000, China

<sup>b</sup> Ministry of Education Key Laboratory of Analytical Science for Food Safety and Biology, Fujian Provincial Key Laboratory of Analysis and Detection Technology for Food Safety, College of Chemistry, Fuzhou University, Fuzhou, Fujian, 350116, China

<sup>c</sup> Hebi Polytechnic, Hebi, Henan 458000, China

<sup>d</sup> Fujian Provincial Key Laboratory of Pollution Monitoring and Control, Fujian Provincial Key Laboratory of Modern Analytical Science and Separation Technology, College of Chemistry, Chemical Engineering and Environment, Minnan Normal University, Zhangzhou, 363000, China.

● **Corresponding author:** Guorong Li, Xiaoyang Pan, Zian Lin;

● **Postal address:** College of Chemistry, Fuzhou University, Fuzhou, Fujian 350108, China

● **Fax:** 86-591-22866135

**E-mail:** 23008@qztc.edu.cn (G. Li), xypan@qztc.edu.cn (X. Pan), zianlin@fzu.edu.cn (Z. Lin);

## 1. Supplementary Methods

### Materials and Reagents

[1,10]phenanthroline-2,9-dicarbaldehyde (PD) was bought from Chemsoon Co., Ltd. 1,3,6,8-tetrakis(4-aminophenyl)pyrene (Py) were purchased from Jilin Chinese Academy of Sciences-Yanshen Technology Co., Ltd. 3,3',5,5'- tetramethylbenzidine (TMB) was purchased from Macklin. Superoxide dismutase (SOD) and catalase (CAT) were obtained from Shanghai Yuanye Bio-Technology Co., Ltd. Terephthalaldehyde (1P), Isoniazid (INH), thiourea, Ethylenediaminetetraacetic acid (EDTA),  $\text{NaN}_3$ , acetic acid (HAc), Tetrabutylammonium hexafluorophosphate ( $\text{Bu}_4\text{NPF}_6$ ),  $\text{ZnCl}_2$ ,  $\text{Na}_2\text{CO}_3$ ,  $\text{CaCl}_2$ ,  $\text{NaNO}_3$ , arginine (Arg), threonine (Thr), phenylalanine (Phe), histidine (His)), glucose (Glu), and ascorbic acid (AA) were purchased from Aladdin Chemistry Co., Ltd (Shanghai, China). Deionized water ( $18.2 \text{ M}\Omega \text{ cm}^{-1}$ ) was produced by Milli-Q water purification system (Millipore, USA).

### Instrumentation

Powder X-ray diffraction (PXRD) measurements were characterized on a CEM DY5261/Xpert3 X-ray diffractometer, and the corresponding data were collected in the range of  $2\theta = 1-30^\circ$  at a scan rate of  $5^\circ/\text{min}$ . Fourier transformed infrared (FT-IR) spectra were acquired with a BD FACSCanto (TM) II spectrometer. X-ray photoelectron spectroscopy (XPS) data was collected by an ESCALAB 250 X-ray photoelectron spectrometer (USA, VG). Solid-state  $^{13}\text{C}$  crosspolarization with magic-angle spinning (CP-MAS) NMR spectrum were recorded on a Bruker Avance NEO 500 MHz spectrometer. Transmission electron microscopy (TEM) images were collected

with Hitachi HT7700 operated at an accelerating voltage of 100 kV. Field emission scanning electron microscopies (SEM) images were obtained by a FEI Nova NanoSEM 230 microscope equipment. Size distribution and zeta potential of Py-PD COF dispersion solutions were collected by a Nano-ZS90 zetasizer (UK, Malvern). N<sub>2</sub> adsorption-desorption isotherms were measured on a Micromeritics ASAP 2020 automatic volumetric instrument at 77 K. The sample was degassed at 120 °C for 8 h under vacuum before measurement. The surface areas were calculated from the adsorption data using brunauer-emmett-teller (BET) model. The pore-size-distribution curve were obtained using the non-localized density functional theory (NLDFT). Thermogravimetric analysis (TGA) was carried out on a STA449C/6/G analyzer from 30 to 1000 °C under Ar<sub>2</sub> atmosphere with a ramp rate of 10 °C/min. The UV-visible (UV-vis) diffuse reflectance spectra (DRS) of solid samples were conducted on a Varian Cary 500 Scan UV-vis spectrophotometer with barium sulfate as the reference. The photoluminescence (PL) measurements were carried out using a FLS920 steady state with a laser ( $\lambda = 345$  nm) at room temperature (UK, Edinburgh). The electron paramagnetic resonance (EPR) spectrum was detected by a Bruker EMX PLUS spectrometer. The white light LED (10 W, 450 nm, Sichuan Yuese Electronic Technology Co. Ltd., China) was employed for the irradiation source with a distance of 10 cm. The absorption spectrum of oxTMB was recorded by a spark microplate reader (Switzerland, Tecan) and the absorbance at 650 nm was used for quantitative analysis.

The cyclic voltammetry (CV) measurement (CHI660D Electrochemical

Workstation, Chenhua Instruments, Shanghai, China) was performed in the classical three-electrode system consisting of COFs modified glassy carbon electrode as the working electrode, a platinum wire as the counter electrode, and an Ag/AgCl electrode as the reference electrode, respectively. A COF material (1 mg) was dispersed in a mixture of ethanol (1 mL) and Nafion D-520 (10  $\mu$ L) to form a homogeneous slurry and then casted onto the pretreated glassy carbon electrode (GCE) surface. The electrolyte was a 0.1 M  $\text{Bu}_4\text{NPF}_6$  acetonitrile solution.  $\text{CH}_3\text{CN}$  solution having tetrabutylammonium hexafluorophosphate ( $\text{Bu}_4\text{NPF}_6$ ) (0.1 mol/L) as electrolyte and 0.01 M ferrocene ( $\text{Fc}/\text{Fc}^+$ ) as internal standard at room temperature. The highest occupied molecular orbital (HOMO) and lowest unoccupied molecular orbital (LUMO) energy levels were calculated by the voltammograms.<sup>1, 2</sup> The  $E_{\text{HOMO}}$  and  $E_{\text{LUMO}}$  were determined as follows:

$$E_{\text{HOMO}} = -(E_{\text{ox}} + 4.4) \text{ eV} \quad \text{Eq. (1)}$$

$$E_{\text{LUMO}} = -(E_{\text{red}} + 4.4) \text{ eV} \quad \text{Eq. (2)}$$

The electrochemically determined band gap were deduced from the difference between onset potentials from oxidation and reduction of copolymers as refer to eq:

$$E_{\text{g}} = E_{\text{ox}} - E_{\text{red}} \text{ eV} \quad \text{Eq. (3)}$$

The results were shown in Supplementary Fig. S7 and Table S2.

Photoelectrochemical measurements were performed in a three-electrode cell using Pt electrode as counter electrode and Ag/AgCl electrode as the reference electrode. A COF material (1 mg) was dispersed in a mixture of ethanol (1 mL) and Nafion D-520 (10  $\mu$ L) to form a homogeneous slurry. Then the catalyst suspension (10

$\mu\text{L}$ ) was dropped onto the ITO glass ( $1\text{ cm} \times 0.3\text{ cm}$ ) surface, forming a film after drying naturally for 12 h. The electrolyte was 0.1 mol/L  $\text{Na}_2\text{SO}_4$  aqueous solution and a 300 W xenon lamp with a cutoff filter ( $\lambda > 420\text{ nm}$ ) was served as the light source. The electrochemical impedance spectroscopy (EIS) and mott-schottky (MS) plots were conducted in a three-electrode system. An aqueous solution containing 0.2 mol/L  $\text{Na}_2\text{SO}_4$  was used as the electrolyte. The EIS was performed in the frequency range from 0.01 Hz to 100 kHz under open circuit potential condition. The MS plots were obtained at 1 kHz, 2 kHz, and 3 kHz.

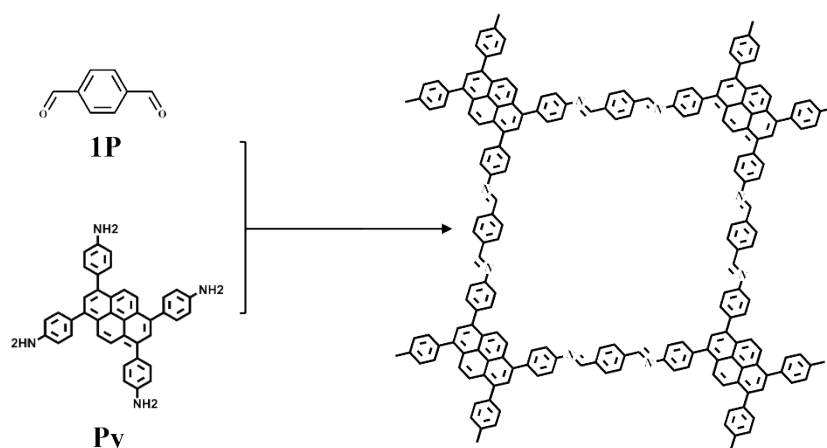
### **Synthesis of Py-PD COF**

PD (11.82 mg, 0.05 mmol) and Py (14.17 mg, 0.025 mmol) were placed into a 10 mL Pyrex tube, and dissolved into 1,2-dichlorobenzene (o-DCB, 0.5 mL) and n-butanol (0.5 mL) mixed solution (v/v = 1:1). After the above mixture was sonicated for 10 min, HAc aqueous solution (0.1 mL, 6 M) was added, and then the system was sonicated again for 2 min. The tube was degassed by three freeze-pump-thaw cycles and then sealed off and heated at 120 °C for 3 days. The powder collected was washed with tetrahydrofuran, acetone, and ethanol several times, and dried at 60 °C under vacuum for 12 h.

### **Synthesis of Py-1P COF**

Py (14.17 mg, 0.025 mmol) and 1P (6.7 mg, 0.05 mmol) were placed into a 10 mL Pyrex tube, and dissolved into the mixed solvent of mesitylene/1,4-dioxane (1 mL, v/v = 3:1). After the above mixture was sonicated for 10 min, HAc aqueous solution (0.1 mL, 6 M) was added, and then the system was sonicated again for 2 min. The tube was

degassed by three freeze-pump-thaw cycles and then sealed off and heated at 120 °C for 3 days. The powder collected was washed with tetrahydrofuran, acetone, and ethanol several times, and dried at 60 °C under vacuum for 12 h.



### The oxidase-like catalytic activity of the COFs

COFs suspension (2 mg/mL, 20  $\mu$ L), acetate buffer (pH 4, 0.2 mmol, 430  $\mu$ L), and TMB (40 mmol, 50  $\mu$ L) were mixed. The mixture was irradiated for 5 min by the visible light. Finally, the mixture was centrifuged at 10000 rpm for 0.5 min. The absorbance at 650 nm of the supernatants were measured to calculate the catalytic activities.

### The kinetic parameters of Py-PD COF nanozyme

The steady-state catalytic kinetics experiments (Michaelis-Menten constants ( $K_m$ )) was performed by varying the concentration of TMB. The Michaelis-Menten equation was applied to describe the rate of enzymatic catalytic reactions Eq. (1):

$$V = V_{max} \times [S]/(K_m + [S])$$

Where  $V$  is the initial velocity,  $[S]$  is the concentration of the substrate,  $V_{max}$  represents the maximal reaction velocity, and  $K_m$  represents the Michaelis constant.

### **Colorimetric detection of INH**

An array of concentrations of INH solution (50  $\mu\text{L}$ ) were added to the reaction system having TMB (40 mmol, 50  $\mu\text{L}$ ), Py-PD COF suspension (2 mg/mL, 20  $\mu\text{L}$ ), and acetate buffer (pH 4, 0.2 mmol), with a final total volume of 500  $\mu\text{L}$ . LED was adapted to illuminate the reaction solution for 5 min to trigger the redox reaction between dissolved oxygen and TMB. The supernatant was obtained after centrifuging at 10000 rpm for 0.5 min. After that, the absorbance change at 650 nm were measured for construct of INH concentration-dependent corresponding curves.

### **Real sample preparation and analysis.**

For determination of INH in healthy human serum (donated from The Third Hospital of Zhangzhou, China), the collected samples were stored at  $-20\text{ }^{\circ}\text{C}$  and thawed at room temperature before further preparation. Three fresh human serum samples with 100-fold dilution were spiked with different amounts of INH to simulate the complex human matrix. The absorbance measurement was performed as described in the aforementioned experiment.

### **DFT calculation**

The first-principles density functional theory (DFT) calculations were calculated with vienna ab initio simulation package (VASP). For the exchange-correlation energy, the perdue-burke-ernzerhof (PBE) version of the generalized gradient approximation (GGA) was generated. A plane wave cutoff energy of 300 eV was used for the plane-wave expansion of the wave function. The energy and force were less than  $10^{-4}$  eV and

$2 \times 10^{-2}$  eV/Å, respectively. The  $k$ -point meshes for the Brillouin zone were sampled in  $2 \times 2 \times 2$  Monkhorst-Pack grid. A vacuum of 15 Å between the layers was considered to safely avoid the interaction between the periodically repeated structures. Optimized lattice parameters for Py-PD COF were  $a = 36.254$  Å,  $b = 35.755$  Å,  $c = 3.853$  Å,  $\alpha = 90^\circ$ ,  $\beta = 74.6^\circ$ ,  $\gamma = 90^\circ$  (Py-1P COF,  $a = 34.914$  Å,  $b = 34.560$  Å,  $c = 3.600$  Å,  $\alpha = 90^\circ$ ,  $\beta = 90^\circ$ ,  $\gamma = 90^\circ$ )



## 2. Supplementary Figures and Tables

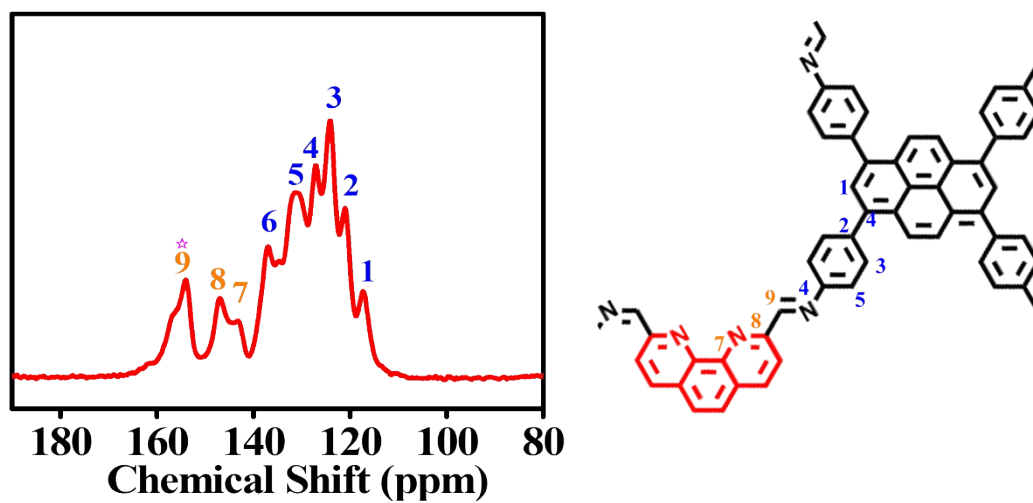


**Fig. S1.** Solid-state  $^{13}\text{C}$  CP-MAS NMR spectrum of Py-PD COF

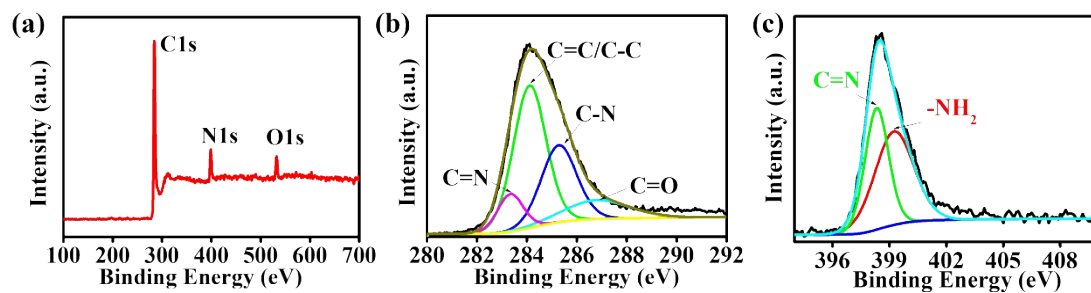


**Fig. S2.** (a) XPS survey, (b) C1s, and (c) N1s spectra of Py-PD COF. The C1s XPS spectrum could be divided into several major peaks centered at around 283.34 eV, 284.15 eV, 285.28 eV, and 286.90 eV which correspond to the C=N, C-C/C=C, C-N, and C=O, respectively. Similarly, the N1s XPS spectrum at around 399.30 and 398.45 eV were ascribed to the N of the unreacted NH<sub>2</sub> groups in Py and C=N bonding structure.

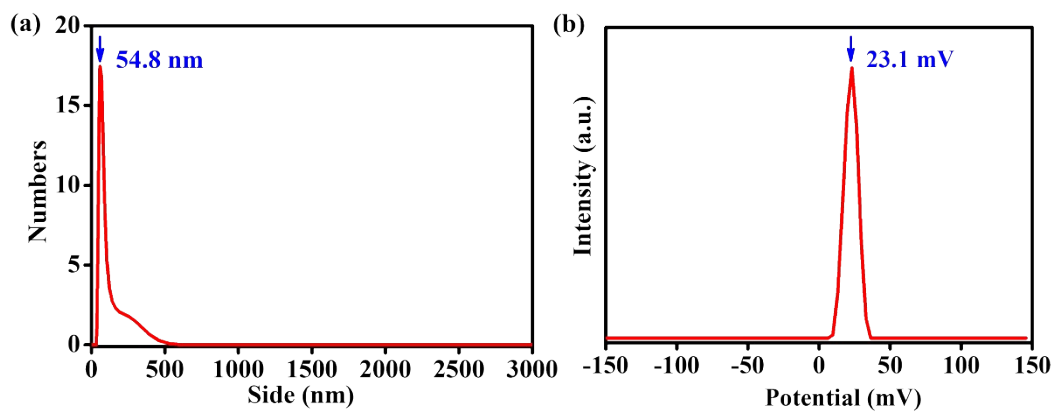


**Fig. S3.** Particle size distribution and zeta potential of Py-PD COF.

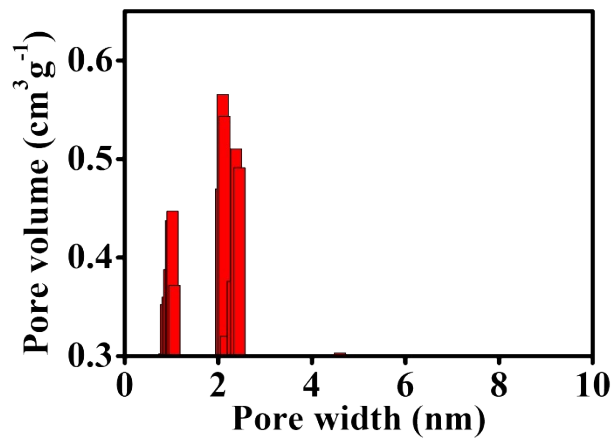


**Fig. S4.** The pore-size distribution of Py-PD COF

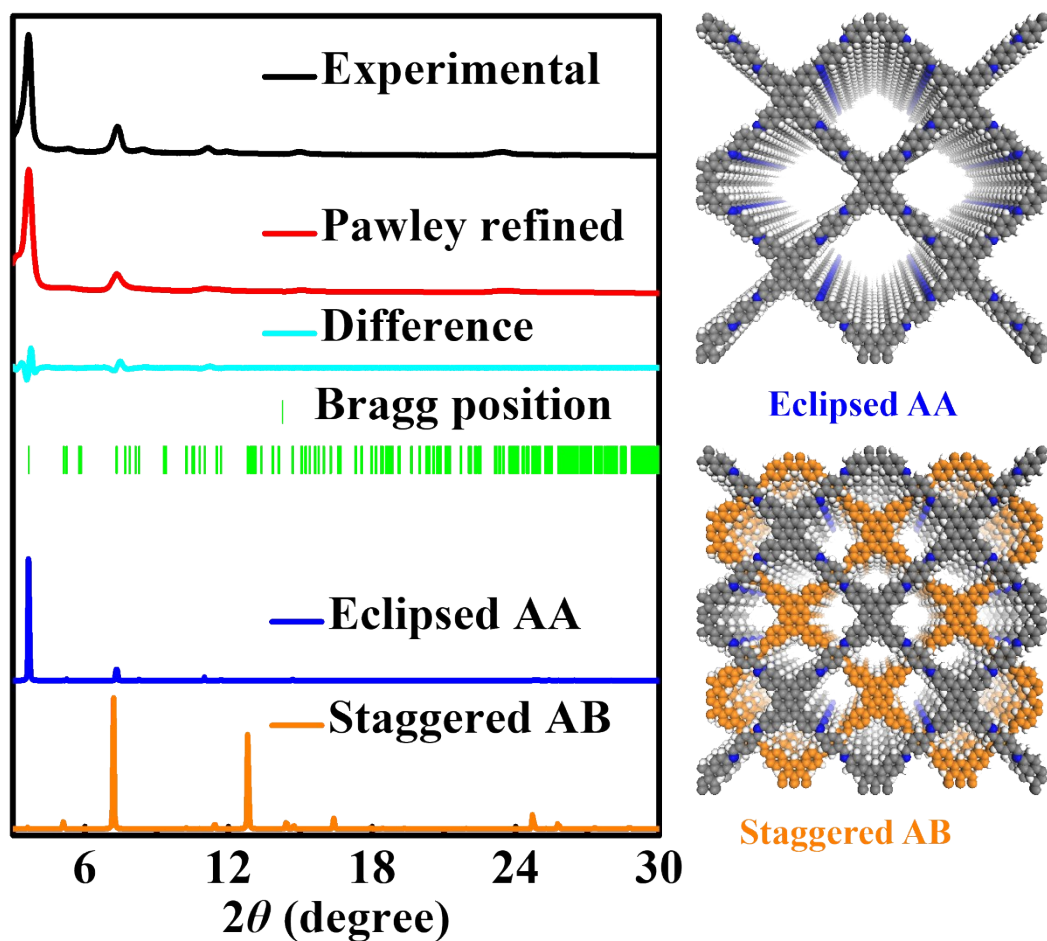


**Fig. S5.** PXRD patterns of Py-1P COF, with top and side views of the corresponding refined eclipsed AA stacking and staggered AB stacking structure. The obtained PXRD data were performed by Pawley refinement.

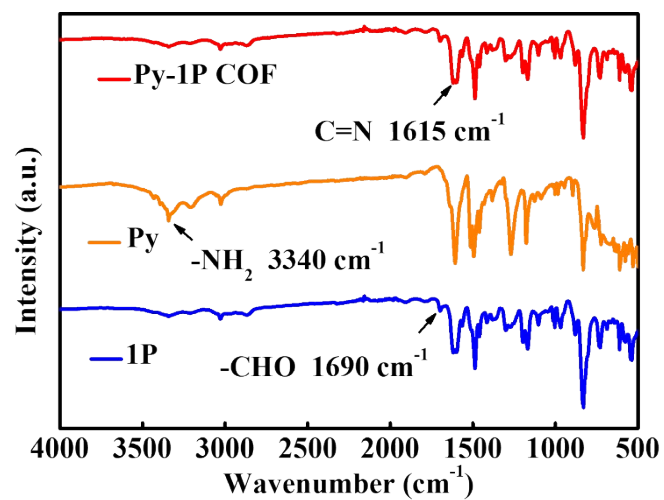


**Fig. S6.** FT-IR analysis of Py-PD COF and its precursors. The peak at  $1615 \text{ cm}^{-1}$  in FT-IR can be attributed to the C=N stretching vibration, indicating the formation of the COF linking unit.

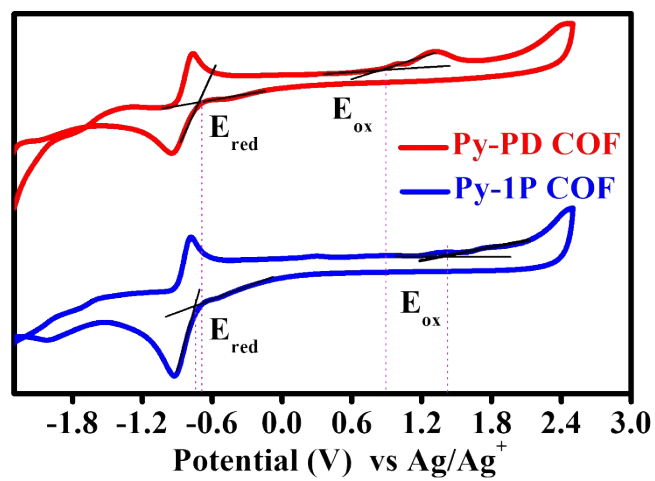


**Fig. S7.** CV of the Py-PD COF and Py-1P COF measured in a 0.1 M Bu<sub>4</sub>NPF<sub>6</sub>-CH<sub>3</sub>CN solutions.

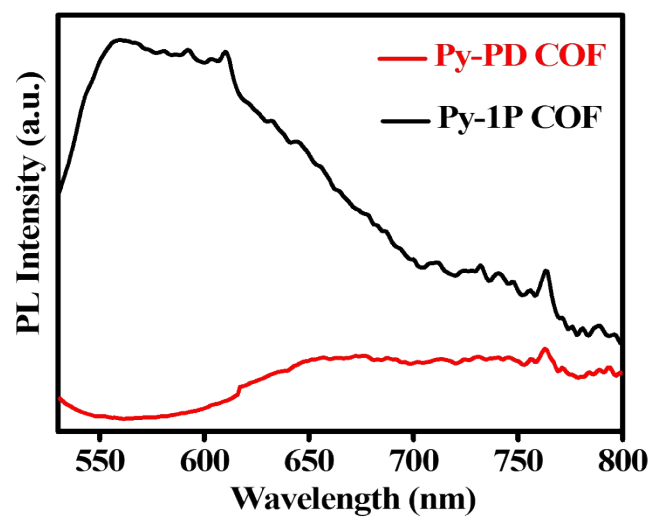


**Fig. S8.** PL spectra of Py-PD COF and Py-1P COF.



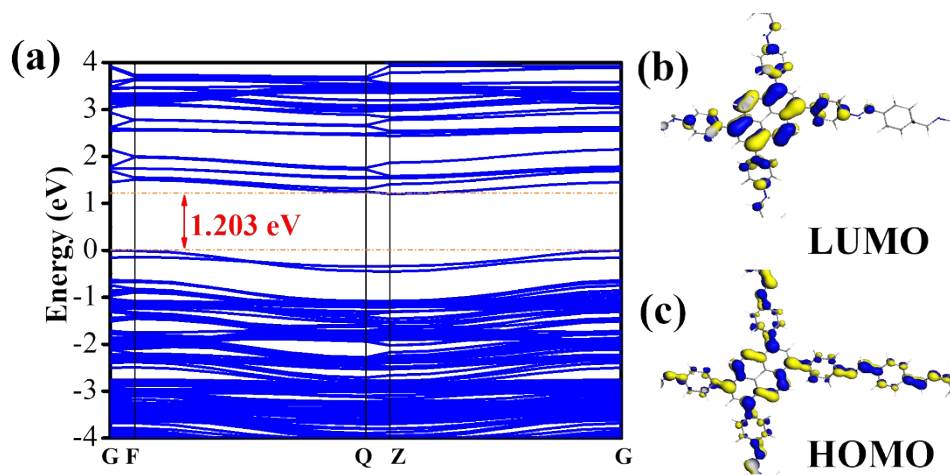


**Fig. S9.** (a) Band structures and visualization of (b) LUMO and (c) HOMO for Py-1P COF.

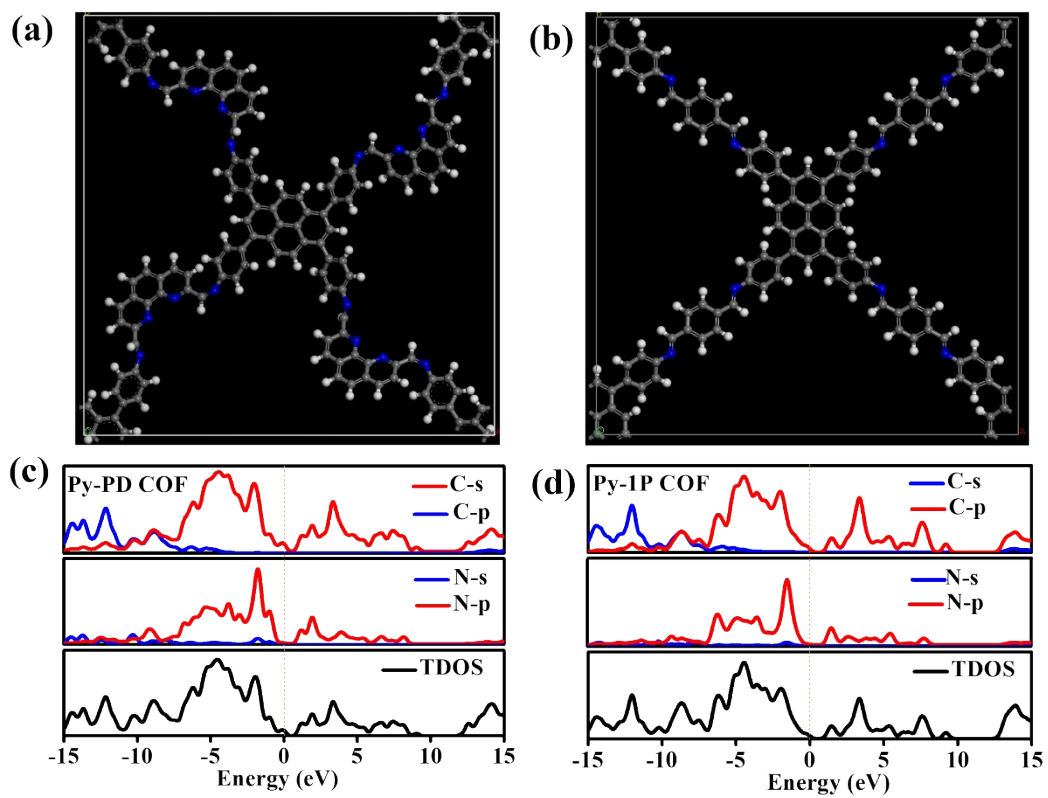


**Fig. S10.** Optimized unit cell of (a) Py-PD COF and (b) Py-1P COF, total density of states (DOS) and orbital-resolved partial DOS of (c) Py-PD COF and (d) Py-1P COF.

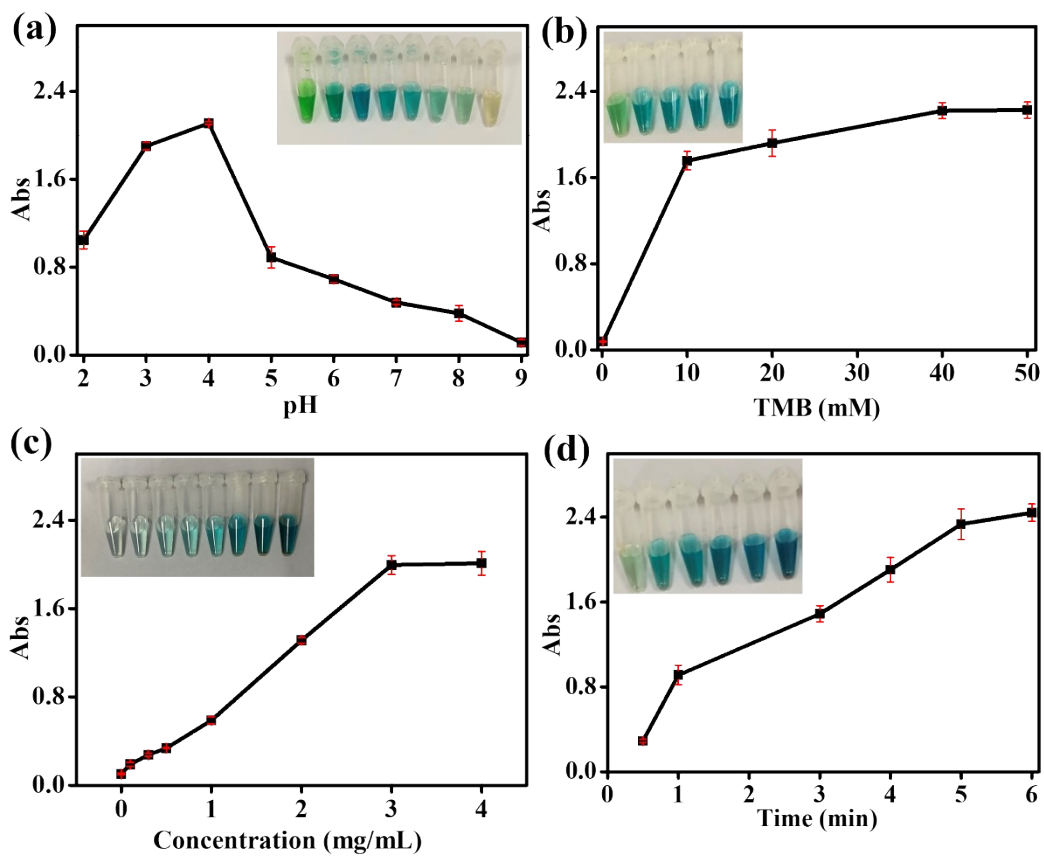


**Fig. S11.** Effects of (a) pH, (b) TMB concentration, (c) Py-PD COF concentration, and (d) light irradiation time. Inset: corresponding photograph.

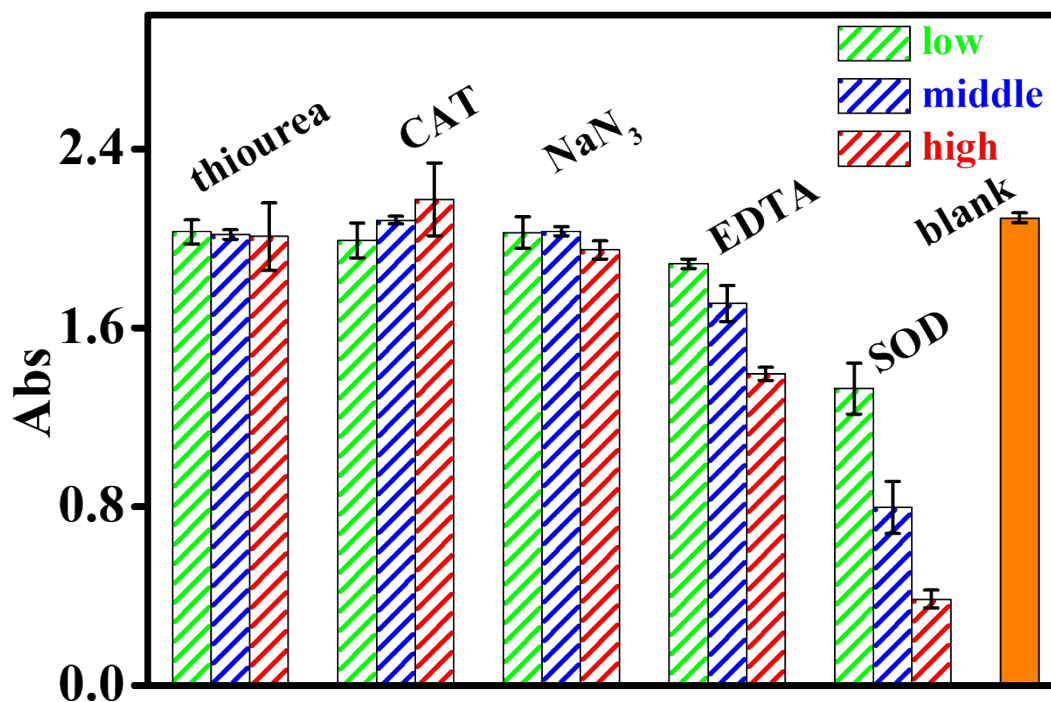


**Fig. S12.** Effect of radical scavengers on the light responsive oxidase like activity of Py-PD COF. SOD (0.5, 1.25, 3.0 mg/mL); EDTA (2.0, 5.0, 10.0 mmol/L); CAT (0.1, 0.5, 2 mg/mL); thiourea (2.0, 5.0, 10.0 mmol/L); NaN<sub>3</sub> (2.0, 5.0, 10.0 mmol/L)

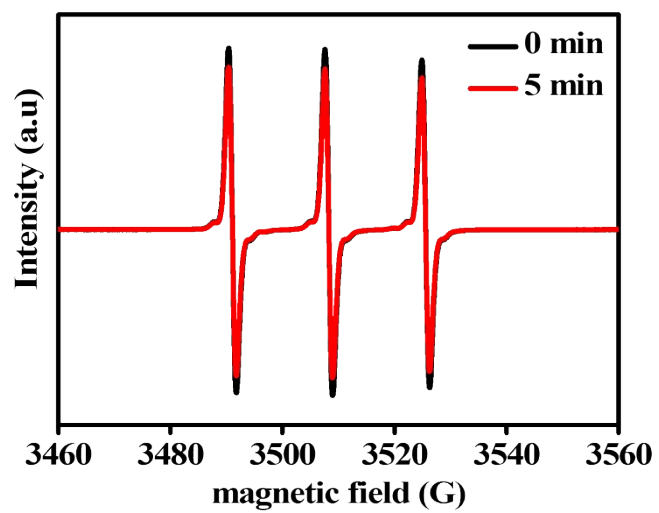


**Fig. S13.** EPR spectra of  $h^+$  trapped by TEMPO.

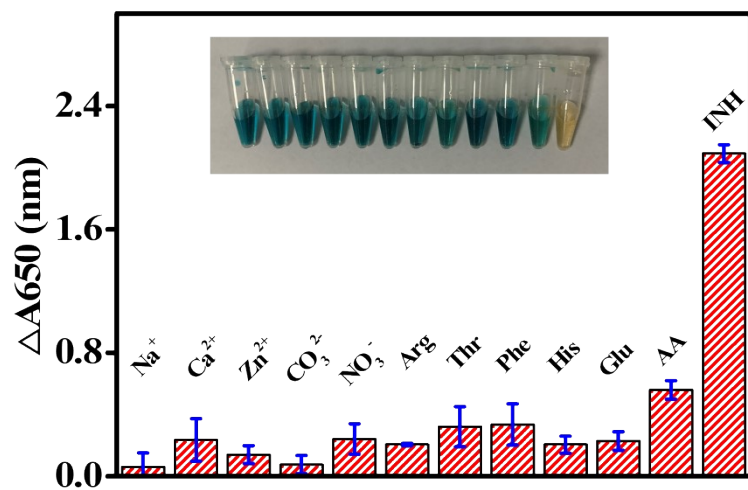


**Fig. S14.** Interference of different reducing agents for detection of INH. The concentration of the interferent was two times than that of INH. Inset: the color change.

**Table S1.** Atomistic coordinates for the Pawley-refined AA mode of Py-PD COF optimized.

---

Space group: P1

Calculated unit cell: a= 36.2541 Å    b= 35.7548 Å    c= 3.8525 Å

$\alpha= 90^\circ$      $\beta= 74.59^\circ$      $\gamma= 90^\circ$

---

H	0.47427	0.60177	0.54793	C	-0.17067	0.08302	0.47742
H	0.57426	0.59095	-0.15901	C	-0.14965	0.05287	0.55359
H	0.61049	0.64947	-0.20862	C	0.57419	0.45963	0.27782
H	0.68854	0.59719	0.31681	C	0.53368	0.46424	0.41388
H	0.65117	0.53936	0.37918	C	0.50804	0.43318	0.51218
H	0.70289	0.70705	0.10275	C	0.59195	0.42162	0.23307
H	-0.05513	0.07978	0.94316	C	0.39108	0.41186	1.03956
H	0.04247	0.08986	1.22122	C	0.36678	0.38158	1.05072
H	0.0621	0.1553	1.22284	C	0.33212	0.38461	0.94829
H	0.16007	0.13295	0.32842	C	0.3216	0.42119	0.87089
H	0.13808	0.06804	0.30703	C	0.34716	0.45084	0.83821
H	0.17138	0.2012	0.78749	C	0.28234	0.33865	0.86192
H	0.54174	0.59409	0.37441	C	0.08246	-0.03007	0.51655
H	0.43897	0.61537	1.0322	C	0.04544	-0.03318	0.44964
H	0.41473	0.67737	0.93135	C	0.03135	-0.0642	0.30626

H 0.327	0.62574	0.5264	C 0.10768	-0.06279	0.52861
H 0.35387	0.56392	0.59225	C -0.07124	-0.10514	0.09581
H 0.35978	0.72205	1.05552	C -0.08264	-0.14186	0.07425
H 0.01127	0.08963	0.86869	C -0.11636	-0.15567	0.31457
H -0.06718	0.09881	0.53257	C -0.13896	-0.1306	0.56541
H -0.10461	0.15137	0.44032	C -0.12627	-0.094	0.59292
H -0.19851	0.07774	0.43061	C 0.41117	0.4786	0.82246
H -0.16328	0.02552	0.58038	C 0.45161	0.47372	0.68346
H 0.51915	0.40489	0.49749	C 0.46929	0.43761	0.62446
H 0.41588	0.40821	1.14414	C 0.38349	0.44688	0.90287
H 0.37439	0.3546	1.14223	C 0.57481	0.39149	0.09631
H 0.29365	0.42727	0.83478	C 0.58589	0.35483	0.12922
H 0.33874	0.47776	0.75199	C 0.61636	0.34648	0.28203
H 0.27637	0.30843	0.91783	C 0.63742	0.37677	0.36765
H 0.05042	-0.08639	0.17615	C 0.62498	0.4135	0.34703
H -0.04611	-0.0952	-0.10425	C -0.07462	-0.04405	0.43627
H -0.06591	-0.16014	-0.13413	C -0.03528	-0.0406	0.42985
H -0.16522	-0.14034	0.75286	C -0.00779	-0.0689	0.32778
H -0.14312	-0.07588	0.80292	C -0.09124	-0.0809	0.37095
H 0.45188	0.41254	0.66915	C 0.09338	-0.09988	0.56924
H 0.55195	0.39689	-0.03124	C 0.1152	-0.12997	0.6246
H 0.57082	0.33205	0.03945	C 0.15294	-0.12523	0.65387



H	0.66134	0.37139	0.48147	C	0.16724	-0.08826	0.62933
H	0.63996	0.4361	0.44152	C	0.14548	-0.05841	0.56037
H	-0.01592	-0.09633	0.25379	C	0.20469	-0.1694	0.6882
H	0.0638	-0.10564	0.5788	C	0.59726	0.49169	0.19652
H	0.10274	-0.15782	0.6547	C	0.51716	0.50093	0.45821
H	0.19494	-0.08252	0.6773	C	0.09331	0.00547	0.61791
H	0.15848	-0.0308	0.5384	C	0.01547	-0.00466	0.63339
H	0.20865	-0.19505	0.83571	C	0.3966	0.51525	0.8618
H	0.62803	0.48814	0.08906	C	0.47624	0.50571	0.59562
H	0.12177	0.00867	0.65688	C	-0.09806	-0.01197	0.50227
H	0.00569	-0.01794	0.89977	C	-0.02019	-0.00203	0.4879
H	0.36597	0.5192	0.9741	C	1.75834	-1.84211	-3.3326
H	-0.12654	-0.01507	0.46319	C	1.69325	-1.82629	-3.14892
H	-0.01035	0.01122	0.22139	C	1.79534	-1.83322	-3.59849
H	1.79264	-1.80844	-3.76265	C	1.75221	-1.87379	-3.10122
H	1.77609	-1.89092	-3.07653	C	1.71544	-1.88271	-2.90982
H	1.70985	-1.90743	-2.73861	C	1.6847	-1.85957	-2.93682
H	1.64009	-1.89442	-2.5996	C	1.66209	-1.80102	-3.16704
H	1.58704	-1.85321	-2.65009	C	1.64584	-1.86879	-2.75731
H	1.56414	-1.79564	-2.87868	C	1.62382	-1.8118	-2.98706
H	1.57933	-1.73615	-3.22879	C	1.61652	-1.84594	-2.78505
H	1.67835	-1.6992	-3.6601	C	1.59354	-1.78793	-3.01276

H	1.72483	-2.39266	-4.2905	C	1.64072	-1.74564	-3.37299
H	1.7886	-2.42146	-4.34987	C	1.6019	-1.75523	-3.20543
H	1.85318	-2.41769	-4.23483	C	1.6483	-1.70909	-3.56319
H	1.90215	-2.38096	-4.04491	C	1.73916	-2.34144	-4.04683
H	1.92349	-2.32129	-3.83093	C	1.80239	-2.33543	-4.01035
H	1.91078	-2.25365	-3.68516	C	1.74677	-2.37764	-4.20216
H	1.82327	-2.20089	-3.77848	C	1.78231	-2.39342	-4.23981
H	1.22229	-2.11043	-3.83024	C	1.81084	-2.37301	-4.132
H	1.28771	-2.08663	-4.10591	C	1.83229	-2.31276	-3.92401
H	1.35823	-2.09148	-4.17224	C	1.84749	-2.3889	-4.14487
H	1.4131	-2.12732	-4.08205	C	1.86795	-2.33019	-3.93159
H	1.43885	-2.18384	-3.8492	C	1.87461	-2.36853	-4.04001
H	1.42631	-2.24477	-3.5253	C	1.89634	-2.30851	-3.83499
H	1.08232	-1.75867	-3.39947	C	1.85401	-2.25506	-3.7727
H	1.07128	-1.69134	-3.51366	C	1.88936	-2.27126	-3.75475
H	1.09562	-1.62681	-3.58891	C	1.84964	-2.21375	-3.73593
H	1.14804	-1.58152	-3.62262	C	1.24195	-2.15603	-3.5461
H	1.21551	-1.56921	-3.61884	C	1.30833	-2.16443	-3.67222
H	1.27444	-1.59092	-3.48569	C	1.24686	-2.12436	-3.77766
C	0.41947	0.54723	0.77025	C	1.28329	-2.11141	-3.93547
C	0.45991	0.5425	0.63534	C	1.31522	-2.13066	-3.87724
C	0.48547	0.57355	0.53477	C	1.34078	-2.18641	-3.63025

C	0.40056	0.58459	0.79033	C	1.35363	-2.11757	-4.02143
C	0.59857	0.5924	-0.04441	C	1.37849	-2.17241	-3.78114
C	0.61934	0.62543	-0.07796	C	1.38403	-2.13748	-3.97211
C	0.65217	0.62834	0.05278	C	1.40973	-2.19387	-3.73842
C	0.664	0.59596	0.2048	C	1.36439	-2.24008	-3.41988
C	0.64241	0.56315	0.24375	C	1.40277	-2.22756	-3.55889
C	0.70096	0.67693	0.04287	C	1.13891	-1.74884	-3.32679
C	-0.08708	0.0236	0.60241	C	1.16107	-1.6872	-3.37726
C	-0.05011	0.02656	0.67061	C	1.10382	-1.73761	-3.39513
C	-0.03602	0.05758	0.81403	C	1.09772	-1.70057	-3.45714
C	-0.11182	0.05663	0.58605	C	1.12677	-1.67428	-3.45457
C	0.06724	0.09937	1.01384	C	1.19104	-1.65987	-3.37487
C	0.0786	0.13633	1.01981	C	1.12225	-1.63565	-3.53411
C	0.11167	0.14962	0.76576	C	1.18611	-1.62216	-3.47774
C	0.1342	0.12364	0.52408	C	1.15115	-1.6106	-3.55192
C	0.12155	0.08682	0.51267	C	1.21724	-1.59736	-3.51637
C	0.1442	0.21059	0.73337	C	1.25133	-1.64567	-3.2865
C	0.58216	0.52809	0.23126	C	1.24985	-1.60922	-3.43007
C	0.54173	0.53287	0.36799	N	0.66688	0.66442	0.06942
C	0.5242	0.56907	0.42283	N	0.1163	0.1884	0.72932
C	0.60821	0.56103	0.13636	N	0.36186	0.69186	0.5842
C	0.41569	0.6173	0.90412	N	-0.17142	0.15096	0.32075

C	0.40116	0.65247	0.85935	N	0.31222	0.35074	0.95415
C	0.36983	0.65636	0.71001	N	-0.12192	-0.19454	0.31076
C	0.3519	0.62365	0.63195	N	0.6191	0.30961	0.39604
C	0.36706	0.58862	0.67304	N	0.17007	-0.15678	0.76036
C	0.35993	0.72233	0.76647	N	1.72957	-1.81859	-3.34519
C	0.06982	0.03748	0.68458	N	1.66997	-1.76818	-3.35417
C	0.03052	0.03395	0.69122	N	1.76688	-2.32062	-3.96706
C	0.00307	0.06227	0.79357	N	1.82597	-2.2756	-3.84834
C	0.08669	0.07437	0.74287	N	1.27219	-2.17604	-3.50763
C	-0.09679	0.09346	0.54043	N	1.3343	-2.21981	-3.45049
C	-0.11775	0.12382	0.47578	N	1.16659	-1.72413	-3.31412
C	-0.15544	0.11965	0.44337	N	1.22278	-1.67046	-3.27446

---

**Table S2.** Electrochemical properties of Py-PD COF and Py-1P COF.

	$E_{\text{ox}}$ (eV)	$E_{\text{red}}$ (eV)	$E_{\text{LUMO}}$ (eV)	$E_{\text{HOMO}}$ (eV)	$E_{\text{g}}$ (eV)	optical band gap
Py-PD	1	-0.7	-3.7	-5.4	1.65	1.7
Py-1P	1.4	-0.75	-3.65	-5.8	2.1	2.15

**Table S3.** Kinetics parameters of nanozymes.

Catalyst	Substrate	$K_m$ (mmol/L)	$v_{max}$ (mol L <sup>-1</sup> s <sup>-1</sup> )	Reference
HRP	TMB	0.434	$1 \times 10^{-7}$	3
MoS <sub>2</sub> NPs	TMB	0.525	$5.16 \times 10^{-8}$	4
ATA-based MOF	TMB	0.407	$8.41 \times 10^{-8}$	5
MoS <sub>2</sub> NPs	TMB	0.525	$5.16 \times 10^{-8}$	4
GO-C <sub>3</sub> N <sub>4</sub> -AgBr	TMB	0.53	-	6
MnOOH	TMB	1	$3.33 \times 10^{-7}$	7
CTF-1	TMB	0.40	-	8
PCN-222 (Fe)	TMB	1.63	-	9
CeO <sub>2</sub>	TMB	1.52	$2.5 \times 10^{-7}$	10
Fe-N/C	TMB	0.62	$5.26 \times 10^{-7}$	11
Co <sub>0.6</sub> /NC-700	TMB	0.35	$3.08 \times 10^{-7}$	12
Mn/Fe-MIL(53)-2	TMB	0.34	-	13
<b>Py-PD COF</b>	<b>TMB</b>	<b>0.323</b>	<b><math>4.98 \times 10^{-7}</math></b>	<b>This work</b>

**Table S4.** Comparison of various methods for detection of INH.

Methods	Materials	LOD ( $\mu\text{M}$ )	Linear range ( $\mu\text{M}$ )	Time (min)	Reference
Electrochemical	IC-rGO/GCE	1.2	5-100	-	14
Electrochemical	PdNPs/CILE	-	5-100	-	15
Electrochemical	Rh-modified GC	13.00	70-1300	-	16
Electrochemical	OPPy	3.15	3.99-126	-	17
Amperometry	Cu(II)-NC	2.6	50-500	-	18
Fluorimetry	COF T <sub>2</sub> Dha-Ac	3.8	0-10000	20 min	19
Colorimetry	CuFe-PBA-NC	-	1-100	20 min	20
Colorimetry	Au@NMOF	0.2	0.25-120	15 min	21
Colorimetry	CuO/NiO	0.4	1-20	10 min	22
Colorimetry	CoOOH	4.0	5-100	5 min	23
Colorimetry	HS-PtNPs	1.7	2.5-250	5 min	24
Colorimetry	Py-PD COF	1.26	2-100	5 min	This work

**Table S5.** INH levels assayed by this method.

Samples	Colorimetric output				HPLC	
	added	found	recovery	RSD	found	RSD
	( $\mu\text{M}$ )	( $\mu\text{M}$ )	(%)	(%)	( $\mu\text{M}$ )	(%)
Sample 1	3	3.08	102.7	0.34		
		3.15	105			
		3.70	123.3			
Sample 2	30	31.76	105.9	0.67	29.7	2.6
		29.03	96.8			
		30.75	102.5			
Sample 3	60	60.26	100.4	0.62	58.9	1.6
		60.97	101.6			
		61.49	102.4			



## References

1. Q. Pan, M. Abdellah, Y. Cao, W. Lin, Y. Liu, J. Meng, Q. Zhou, Q. Zhao, X. Yan, Z. Li, H. Cui, H. Cao, W. Fang, D. A. Tanner, M. Abdel-Hafiez, Y. Zhou, T. Pullerits, S. E. Canton, H. Xu and K. Zheng, *Nat. Commun.*, 2022, **13**, 845.
2. C. M. Cardona, W. Li, A. E. Kaifer, D. Stockdale and G. C. Bazan, *Adv. Mater.*, 2011, **23**, 2367-2371.
3. L. Z. Gao, J. Zhuang, L. Nie, J. B. Zhang, Y. Zhang, N. Gu, T. H. Wang, J. Feng, D. L. Yang, S. Perrett and X. Yan, *Nat. Nanotechnol.*, 2007, **2**, 577-583.
4. T. R. Lin, L. S. Zhong, L. Q. Guo, F. F. Fu and G. N. Chen, *Nanoscale*, 2014, **6**, 11856-11862.
5. Y. Nian, L. Luo, W. Zhu, C. Yang, L. Zhang, M. Li, W. Zhang and J. Wang, *Inorg. Chem. Front.*, 2021, **8**, 3482-3490.
6. C. M. Ding, X. Wang, K. J. Song, B. Zhang, J. W. Wang, Z. H. Zhao, H. H. Chang and W. L. Wei, *Sens. Actuators, B: Chem.*, 2018, **268**, 376-382.
7. L. Yu, H. Li, W. Huang, H. Yu and Y. He, *Inorg. Chem.*, 2021, **60**, 5264-5270.
8. J. He, F. Xu, J. Hu, S. Wang, X. Hou and Z. Long, *Microchem. J.*, 2017, **135**, 91-99.
9. D. W. Feng, Z. Y. Gu, J. R. Li, H. L. Jiang, Z. W. Wei and H. C. Zhou, *Angew. Chem. Int. Ed.*, 2012, **51**, 10307-10310.
10. X. Cheng, L. Huang, X. Yang, A. A. Elzatahry, A. Alghamdi and Y. Deng, *J. Colloid Interface Sci.*, 2019, **535**, 425-435.
11. Y. Wang, Z. Zhang, G. Jia, L. Zheng, J. Zhao and X. Cui, *Chem. Commun.*, 2019, **55**, 5271-5274.
12. Y. Li, Y. Lu, X. Zhang, H. Cao and Y. Huang, *ACS Appl. Nano Mater.*, 2021, **4**, 9547-9556.
13. L. Luo, Y. Ou, Y. Yang, G. Liu, Q. Liang, X. Ai, S. Yang, Y. Nian, L. Su and J. Wang, *J. Hazard. Mater.*, 2022, **423**, 127253.

14. L. Qian, A. R. Thiruppathi, J. van der Zalm and A. Chen, *ACS Appl. Nano Mater.*, 2021, **4**, 3696-3706.
15. G. Absalan, M. Akhond, M. Soleimani and H. Ershadifar, *J. Electroanal. Chem.*, 2016, **761**, 1-7.
16. S. Cheemalapati, S.-M. Chen, M. A. Ali and F. M. A. Al-Hemaid, *Toxicol. Appl. Pharmacol.*, 2014, **121**, 444-450.
17. M. R. Majidi, A. Jouyban and K. Asadpour-Zeynali, *J. Electroanal. Chem.*, 2006, **589**, 32-37.
18. A. Safavi, M. A. Karimi, M. R. Hormozi Nezhad, R. Kamali and N. Saghir, *Spectrochim. Acta, Part A*, 2004, **60**, 765-769.
19. Y. Cao, L. Zhang, J. Yang, J. Zhang, W. Si, J. Wang, A. Iqbal, W. Qin and Y. Liu, *Sens. Actuat. B Chem.*, 2021, **346**, 130472.
20. R. P. Ojha, S. Pal and R. Prakash, *Microchem. J.*, 2021, **171**, 106854.
21. J. Yu, Q. Sun, J. Sun, X. Wang, N. Niu and L. Chen, *Sens. Actuat. B Chem.*, 2023, **390**, 134024.
22. W. Zhu, Y. Cheng, C. Wang and X. Lu, *Inorg Chem*, 2022, **61**, 16239-16247.
23. N. Azizi, T. Hallaj and N. Samadi, *Luminescence*, 2022, **37**, 153-160.
24. S. B. He, L. Yang, X. L. Lin, L. M. Chen, H. P. Peng, H. H. Deng, X. H. Xia and W. Chen, *Talanta*, 2020, **211**, 120707.